NUMERICAL MODELING PROCEDURES FOR PRACTICAL COAL MINE DESIGN

By R. Karl Zipf, Jr., Ph.D., P.E.[1]

ABSTRACT

A method is presented for creating realistic numerical models for practical coal mine ground control. The method includes procedures to collect the necessary mechanical input parameters from a geologic core log, procedures to set up a model, and procedures to interpret calculation results. The input parameters come from a detailed geologic core log and extensive point load tests of estimate rock layer strength. A suite of material property input parameters is proposed that allows the user to go from core log to numerical model inputs. Rock bolt anchorage properties are also linked to the material properties of each geologic layer in the model. Following this procedure leads to very realistic calculations of the rock failure process and rock support system behavior. These calculations in turn enable realistic comparison of the effectiveness of alternative rock support systems.

INTRODUCTION

Reducing ground failure fatalities and injuries is a priority of the National Institute for Occupational Safety and Health's (NIOSH) mine safety and health research program. Ground failures have historically accounted for up to 50% of the fatalities in U.S. underground mines, and nonfatal injuries due to ground failure are almost always severe. Ground failures helped trigger recent mine disasters in Alabama (2001) and Utah (2000) by disrupting ventilation that led to gas explosions. Together, these incidents claimed the lives of 15 coal miners. In 2006, 10 underground coal miners lost their lives in 7 roof falls, 2 rib rolls, and 1 coal mine bump.

To reduce fatalities and injuries due to ground failure, NIOSH researchers are working toward improved understanding of rock mass failure mechanics using numerical analysis models. Promoting more widespread use of numerical models for ground control engineering may lead to the desired safety improvements; however, several barriers exist toward that end. Considerable guidance is needed for collecting necessary input data, setting up a model, and finally interpreting the analysis results. Such guidance should have the agreement of all parties involved in practical ground control, including mining companies, consultants, suppliers, and regulatory authorities. To enable better communication among mining engineers working in coal mine ground control, NIOSH researchers have made progress toward a set of input parameters for use in FLAC[2] [Itasca Consulting Group 1994] that result in very realistic models of coal mine rock behavior and rock bolts. Finally, the suggested guidance is not intended as a substitute for sound engineering judgment.

Obtaining the input parameters requires collection of certain information from rock core. The input parameters include material properties for a strain-softening, ubiquitous-joint constitutive model, rock bolt properties, and model initialization and loading. Use of these input parameters seems to lead automatically to (1) realistic modeling of the failure mechanics, (2) calculation of displacement and stress that are consistent with field measurements, and (3) a reasonable forecast of the effectiveness of rock support alternatives. This paper discusses a core logging procedure to obtain numerical model input parameters, presents a suite of input parameters for practical coal mine models, and demonstrates their use with a practical example.

CORE LOGGING FOR INPUT PARAMETERS

Obtaining meaningful results from a numerical model begins with the collection of adequate geologic information. The method described for translating a geologic core log into input parameters for a numerical model follows a philosophy developed by Gale and Tarrant [1997] of "letting the rocks tell us their behavior." For numerical modeling of coal mines, the logger must record two essential details, namely, individual geologic layers of homogeneous character and the strength of those geologic layers. Figure 1 shows a typical section of core with several distinct layers and other essential features to record.

The logging detail necessary depends on the scale of the numerical model. Small-scale models of coal mine entry behavior may require logging geologic layers as small as 50 mm. Larger-scale coal mine models for subsidence prediction may require less logging detail. Of particular importance to note are the soft clay layers or major bedding planes with weak infilling as indicated in Figure 1.

Having defined the geologic layering in sufficient detail, the logger must next estimate the strength of those layers, including the strength of the rock material and the strength of bedding plane discontinuities. Uniaxial compressive strength (UCS) tests, triaxial tests, or multistage

---

Figure 1.—Photograph of core showing different rock layers and a prominent clay layer from 1.4 to 1.5 ft.

triaxial tests on core specimens oriented both perpendicular to bedding and at a 30° angle to bedding are the best way to measure cohesion and friction angle for the rock material and bedding plane discontinuities. However, conducting extensive tests is rarely a feasible option. Index tests are the preferred option and have the distinct advantage of providing multiple strength estimates for each geologic layer. Basic soil and rock descriptions of the International Society for Rock Mechanics [ISRM 1981] can provide a crude estimate of strength. Other options include simple hammer blow tests [ISRM 1981; Molinda and Mark 1996] or the Schmidt Hammer test for stronger materials [ISRM 1993]. The Point Load Index [ISRM 1985] seems to be the simplest and most reliable method at present to estimate rock material and bedding plane strength through an axial or diametral point load test, respectively. Based upon thousands of tests, reliable correlations between Point Load Index and UCS have been developed for a variety of coal mine rocks throughout the United States [Rusnak and Mark 2000]. Techniques to estimate rock layer strength based on downhole geophysical measurements are also well developed [Medhurst and Hatherly 2005]; however, the methods have never been adopted widely by the U.S. coal industry. Figure 2 shows estimates of the rock material and bedding plane strength for each geologic layer based on point load tests.
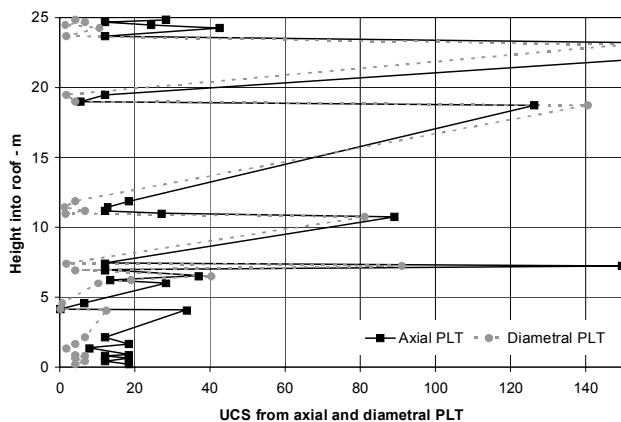

Figure 2.—Typical strength data along rock core from axial and diametral point load tests (PLT).

Detailed geologic logging for numerical modeling purposes has a relation to the Coal Mine Roof Rating (CMRR) used to describe coal mine roof rock in practical ground control [Mark et al. 2002b]. The CMRR Unit Rating for each rock layer is composed of two parts. The UCS rating for the rock material strength ranges from 5 to 30 for a range of strengths between 0 and 138 MPa as determined from axial point load tests. The discontinuity rating for the bedding plane strength ranges from 25 to 60 corresponding to strength of about 6–52 MPa based on diametral point load tests.

MATERIAL PROPERTIES

For general modeling of rock behavior in coal mine ground control, the FLAC program [Itasca Consulting Group 1994] contains many useful features, in particular, the SU constitutive model. "SU" stands for the strain-softening, ubiquitous-joint model and is ideal for simulating laminated coal measure rocks. In essence, this constitutive model allows for strain-softening behavior of the rock matrix and/or failure along a predefined weakness plane such as bedding planes. Failure through the rock matrix or along a bedding plane can occur via shear or tension, and the dominant failure mode can change at any time. The "state" variable within FLAC tracks the failure mode in each model element as either shear or tensile failure through the rock matrix or along a bedding plane.

The SU constitutive model requires four major input parameters, namely, cohesion, friction angle, dilation angle, and tensile strength for both the rock matrix and the bedding planes. Based on a Mohr-Coulomb strength model, the UCS of a rock depends on cohesion and friction angle as

$$UCS = \frac{2\,c\,\cos\phi}{1-\sin\phi} \qquad (1)$$

where c is the cohesion and φ is the friction angle. Careful geologic core logging along with point load testing to estimate the UCS of each rock layer provides a rational basis to estimate the most important input parameters to the SU constitutive model.

Tables 1 and 2 summarize the name, UCS, and the initial value for input parameters of a proposed suite of "numerical rocks," along with a corresponding geologic description of the rock. The UCS values indicated in Tables 1 and 2 are field-scale or model-scale values that are reduced from the laboratory-scale values determined from point load tests during geologic logging. Following the lead of Gale and Tarrant [1997] again, these laboratory values of UCS for rock and coal, but not soil, are reduced by a factor of 0.56 to produce the field-scale UCS and hence the input parameters to the numerical model. This scaling factor works well for rock masses associated with coal mining; however, it does not apply outside this narrow scope.

Table 1.—Initial values for rock material input parameters

Material name	Description	Lab UCS (MPa)	Field UCS (MPa)	Young's modulus (GPa)	Cohesion (MPa)	Friction angle, °	Dilation angle, °	Tensile strength (MPa)
Soil 1...................	Paste	0.04	0.02	1	0.007	21	10	0.002
Soil 2...................	Very soft soil	0.07	0.04	1	0.014	21	10	0.004
Soil 3...................	Soft soil	0.14	0.08	1	0.028	21	10	0.008
Soil 4...................	Firm soil	0.29	0.16	1.5	0.055	21	10	0.016
Soil 5...................	Stiff soil	0.63	0.35	2	0.120	21	10	0.035
Soil 6...................	Very stiff soil	3.6	2.0	2.5	0.69	21	10	0.20
Rock 1	Claystone, fireclay	6.4	3.6	3	1.2	22	10	0.3
Rock 2	Black shale	11	6	4	2.0	23	10	0.6
Rock 3	Black shale, gray shale	18	10	5	3.3	24	10	1.0
Rock 4	Gray shale	25	14	6	4.5	25	10	1.4
Rock 5	Siltstone, gray shale	34	19	7	6	26	10	1.9
Rock 6	Siltstone	48	27	8	8	28	10	2.7
Rock 7	Siltstone, sandstone	63	35	10	10	30	10	3.5
Rock 8	Sandstone, limestone	77	43	12	12	32	10	4.2
Rock 9	Sandstone	95	53	15	14	34	10	5.2
Rock 10	Limestone	139	78	20	20	36	10	7.7
Coal 1	Banded, bright coal	3.6	2.0	2.5	0.6	29	10	0.17
Coal 2	Banded coal	6.3	3.5	2.5	1.0	30	10	0.29
Coal 3	Banded, dull coal	12	6.7	2.5	1.9	31	10	0.60
Coal 4	Dull coal	17	9.7	2.5	2.7	32	10	0.85

Table 2.—Initial values for bedding plane input parameters

Material Name	Description	Lab strength (MPa)	Field strength (MPa)	Young's modulus (GPa)	Cohesion (MPa)	Friction angle, °	Dilation angle, °	Tensile strength (MPa)
Soil 1	Paste	0.04	0.02	1	0.007	21	10	0.002
Soil 2	Very soft soil	0.07	0.04	1	0.014	21	10	0.004
Soil 3	Soft soil	0.14	0.08	1	0.028	21	10	0.008
Soil 4	Firm soil	0.29	0.16	1.5	0.055	21	10	0.016
Soil 5	Stiff soil	0.63	0.35	2	0.120	21	10	0.035
Soil 6	Very stiff soil	1.4	0.80	2.5	0.27	21	10	0.080
Rock 1	Claystone, fireclay	2.7	1.5	3	0.5	21	10	0.15
Rock 2	Black shale	5.4	3.0	4	1.0	22	10	0.30
Rock 3	Black shale, gray shale	10	5.7	5	1.9	23	10	0.60
Rock 4	Gray shale	18	10	6	3.3	24	10	1.0
Rock 5	Siltstone, gray shale	25	14	7	4.5	25	10	1.4
Rock 6	Siltstone	32	18	8	5.5	26	10	1.7
Rock 7	Siltstone, sandstone	41	23	10	7	27	10	2.3
Rock 8	Sandstone, limestone	59	33	12	10	28	10	3.3
Rock 9	Sandstone	86	48	15	14	29	10	4.8
Rock 10	Limestone	123	69	20	20	30	10	6.8
Coal 1	Banded, bright coal	1.6	0.9	2.5	0.3	25	10	0.08
Coal 2	Banded coal	2.9	1.6	2.5	0.5	26	10	0.15
Coal 3	Banded, dull coal	6.4	3.6	2.5	1.1	27	10	0.30
Coal 4	Dull coal	12	6.7	2.5	2.0	28	10	0.60

The material suite shown in Tables 1 and 2 includes very weak soils and claylike materials with a UCS of 0.02 MPa and weak, medium, and strong rocks with a UCS of about 150 MPa. Also included is coal, which ranges from the most friable with a UCS of 2 MPa to a strong coal with a UCS of 12 MPa. The soil material models are isotropic, i.e., the soil matrix properties are the same as those for the horizontal weakness plane. However, the rock models exhibit anisotropy since the strength along bedding planes is less than the UCS of the rock matrix. Following results of point load tests by Molinda and Mark [1996], weak rocks are the most anisotropic, with the strength along bedding planes about 50% of the rock matrix UCS, while stronger rocks have less anisotropy, with the strength along bedding planes about 90% of the rock matrix. The coal models have a similar trend in strength anisotropy, with the stronger coal less anisotropic than the weaker coal. For the stronger coal, the ratio of axial strength to strength parallel to bedding is about 1.5 to 1, whereas for the weaker coal the ratio is about 2.2 to 1. The weaker coal models would apply to more cleated coal, i.e., containing more closely spaced joints. The extensive material property suite for coal mine rocks proposed in Tables 1 and 2 is

generally consistent with a smaller set of properties proposed by Reddish et al. [2000].

Note that in proposing this suite of numerical rock properties, the UCS of the rock matrix is independent from the strength of the bedding planes. In the absence of specific data, the user will usually specify the rock matrix and bedding plane strength as a pair with strength ratio similar to that noted by Molinda and Mark [1996] for an extensive database of axial and diametral point load tests. However, the strength values for the rock matrix and bedding planes are independent in the material property suite, and the user can specify any value for the bedding plane strength up to that of the rock matrix UCS.

In creating the material model suites, friction angle for the matrix and bedding planes are assumed to vary as shown in Tables 1 and 2, respectively. These assumptions for friction angle along with Equation 1 then imply the values for peak cohesion shown in Tables 1 and 2. Thus, the UCS of the rock matrix and the bedding plane strength provide two of the four major input parameters to the SU constitutive model in FLAC.

Assumed friction angle values for the rock matrix ranges are 21° for soil- and claylike materials up to 36° for the strongest rocks. These values may be somewhat low compared to published values of Jaeger and Cook [1979] and Farmer [1968]. Later revisions of this material property suite may include a one friction angle range for application at low confinement and another for application at high confinement. Assumed friction angle values for the bedding plane are 21° for soil- and claylike materials up to 30° for the strongest rocks. These values are consistent with data developed by Barton and summarized by Hoek et al. [1995].

Other major assumptions within this material model suite are as follows:

1. Moduli for the materials range from 1 to 20 GPa. Weaker materials have a lower modulus, while stronger materials have a higher modulus. The ratio of modulus to UCS of the rock matrix varies from about 1,000 for the weakest to about 100 for the strongest materials. The moduli for the material and the modulus-to-UCS ratio are consistent with data shown in Jaeger and Cook [1979] and Gale and Fabjanczyk [1993].
2. Cohesion decreases from its peak value given in Tables 1 and 2 to a residual value of 10% of peak over 5 millistrain of postfailure strain. It is this decrease in cohesion with postfailure strain that gives rise to strain-softening behavior of both the rock matrix and the bedding planes.
3. Friction angle remains constant at the values shown in Tables 1 and 2, even in the postfailure regime.
4. Tensile strength is equal to cohesion for the soil materials and decreases to 0 over 1 millistrain of postfailure strain.

5. Tensile strength values are generally about 10% of UCS. It also decreases to 0 over 1 millistrain of postfailure strain. This strength ratio is again consistent with rock strength data shown in Jaeger and Cook [1979] and Farmer [1968].
6. Dilation angle is initially 10° and decreases to 0° over 5 millistrain of postfailure strain.

ROCK BOLT PROPERTIES

In addition to its robust constitutive models, FLAC includes various structural support elements. The structural element called "cable" represents rock support as an axial force along a line, and this approach suffices for most rock or cable bolts in practical coal mining applications. If the shear or moment resistance of a rock bolt is significant, the "pile" structural element may be a more appropriate choice.

Properties required by the "cable" element are the structural characteristics of the steel, namely, elastic modulus, cross-sectional area, and yield strength, along with the structural characteristics of the anchor. Resin along with some cement grout now dominates most anchors used with rock and cable bolts in U.S. mines [Dolinar and Bhatt 2000]. Two properties represent the anchor characteristics in FLAC: "Kbond," which is the stiffness of the grout, and "Sbond," which is its cohesive strength.

Kbond, or anchorage stiffness, depends on grout properties and the annulus thickness, i.e., hole radius minus bolt radius. Based on numerical studies by St. John and Van Dillen [1983] of the grout-rock interface, the FLAC manuals [Itasca Consulting Group 1994] suggest the following expression for a practical estimate of Kbond for use in FLAC:

$$\text{Kbond} \cong \frac{2\pi G}{10\ln(1 + 2t/D)} \qquad (2)$$

where G is the grout shear modulus, D is the bolt diameter, and t is the annulus thickness.

Farmer [1975] reports a value of 2.25 GPa (455,000 psi) for the Young's modulus of resin grout. For a typical 19-mm (0.75-in) rock bolt in a 28.6-mm (1.125-in) hole, Kbond is approximately 1.4×10^9 N/m/m. Over the practical range of rock bolt and hole diameters and the likely range for grout modulus, Kbond varies at most from about 1 to 2×10^9 N/m/m.

Numerical modeling of laboratory measurements of rock bolt behavior confirms this estimate of Kbond. Numerous researchers [Kwitowski and Wade 1980; Serbousek and Signer 1987; Signer 1990; Tadolini 1986] used strain gauges to measure the load distribution along fully grouted, 1-m-long rock bolts embedded in large blocks of limestone, shale, or concrete. Figure 3 shows

various measured load profiles where the bolt load at zero distance along the bolt is the actual applied load. Note the exponential decay of bolt load with distance, which is consistent with analytical models proposed by Farmer [1975] and Serbousek and Signer [1987]. A simple FLAC model of these laboratory pull tests was used to calculate the bolt load distribution for Kbond values of 0.5, 1, and 2×10^9 N/m/m and an applied load of 60 kN. As seen in Figure 4, Kbond equal to 1×10^9 N/m/m matches the laboratory measurements well.
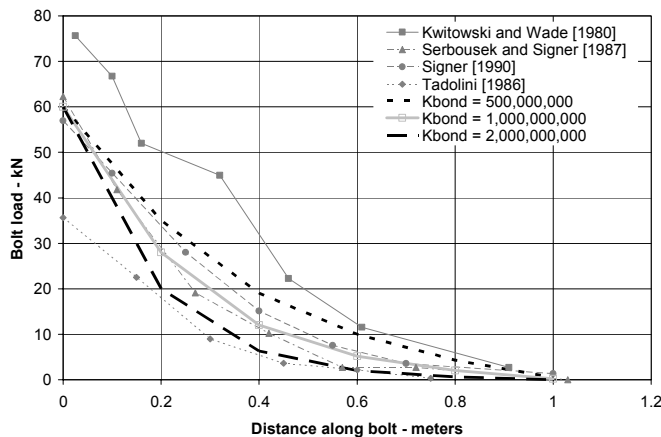

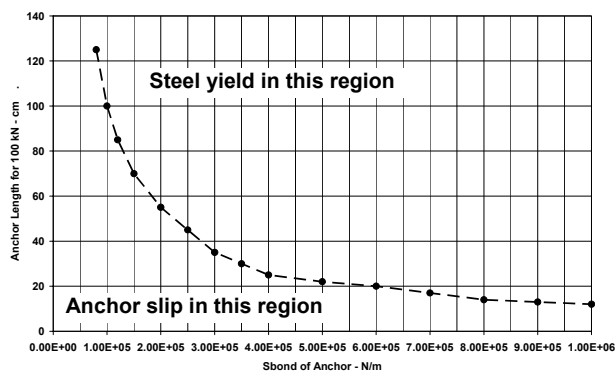**Figure 3.—Measured and calculated load profiles along rock bolts.**

Figure 4.—Anchor length required for 100-kN capacity for various Sbond.

Sbond is also known as bond factor, anchor factor, or grip factor and has a typical value of about 350 kN/m (1 ton/in) in coal mine rocks. Its value depends on the likely failure mode of the bolt anchor. If the grout is weak, shear failure occurs along the bolt-grout interface, and Sbond depends on the grout cohesion and the perimeter of the bolt. Farmer [1975] reports a value of 160 MPa for the compressive strength of resin grout. Assuming that the

cohesion is one-third of this value, Sbond at the bolt-grout interface for a typical 19-mm (0.75-in) bolt is about 3.2 MN/m.

However, in coal mine rocks, shear failure typically occurs along the grout-rock interface, where Sbond depends on the lesser of the rock or grout cohesion and the perimeter of the hole. Table 1 indicates that rock cohesion varies from 1.2 to 20 MPa and is even less for the occasional thin clay layers. Thus, for a hole diameter in the 25- to 35-mm range, Sbond varies from 80 kN/m to 2.2 MN/m (0.2 to 4.5 tons/in) depending on the rock material strength. Table 3 shows the range of Sbond values for various rock materials. For practical coal mine modeling with FLAC, the user should specify bolt sections that correspond to the top and bottom of a geologic layer and then assign an Sbond value for that section consistent with the rock material properties for that layer. Table 4 shows Sbond values for various rocks either measured directly or inferred from select pull test data. Values range from 77 to 1,225 kN/m and are consistent with the Sbond input parameters shown in Table 3. Note that the values for Kbond and Sbond discussed here assume a unit bolt spacing of 1 m between rows of bolts. These rock bolt properties and others require scaling according to the actual rock bolt spacing.

Table 3.—Sbond values for various rock materials

Material name	Description	Cohesion (MPa)	Sbond for 25-mm hole (N/m)	Sbond for 35-mm hole (N/m)
Soil 1	Paste	0.007	559	770
Soil 2	Very soft soil	0.014	1,120	1,540
Soil 3	Soft soil	0.028	2,230	3,080
Soil 4	Firm soil	0.055	4,390	6,050
Soil 5	Stiff soil	0.120	9,580	13,200
Soil 6	Very stiff soil	0.69	55,100	75,900
Rock 1	Claystone, fireclay	1.2	95,800	132,000
Rock 2	Black shale	2.0	160,000	220,000
Rock 3	Black shale, gray shale	3.3	263,000	363,000
Rock 4	Gray shale	4.5	359,000	495,000
Rock 5	Siltstone, gray shale	6	479,000	660,000
Rock 6	Siltstone	8	638,000	880,000
Rock 7	Siltstone, sandstone	10	798,000	1,100,000
Rock 8	Sandstone, limestone	12	958,000	1,320,000
Rock 9	Sandstone	14	1,120,000	1,540,000
Rock 10	Limestone	20	1,600,000	2,200,000
Coal 1	Banded, bright coal	0.6	47,900	66,000
Coal 2	Banded coal	1.0	79,800	110,000
Coal 3	Banded, dull coal	1.9	152,000	209,000
Coal 4	Dull coal	2.7	215,000	297,000

Table 4.—Measured Sbond in various rocks.

Rock	Sbond (N/m)	Reference
Shale-concrete	77,000	Bartels and Pappas [1985].
Plaster	126,000	Bartels and Pappas [1985].
Chalk	193,000	Franklin and Woodfield [1971].
Dark gray fireclay	220,500	Mark et al. [2002a].
Layered dark gray shale.........	252,000	Mark et al. [2002a].
Sandstone	289,000	Franklin and Woodfield [1971].
Concrete blocks...	290,000	Pettibone [1987].
Thinly banded gray shale.........	290,500	Mark et al. [2002a].
Clay, claystone	304,500	Mark et al. [2002a].
Dark gray shale ...	364,000	Mark et al. [2002a].
Coal	385,000	Franklin and Woodfield [1971].
Gypsum	385,000	Dunham [1974].
Limestone...........	400,000	Dunham [1974].
Anhydrite	526,000	Dunham [1974].
Limestone...........	1,225,000	Franklin and Woodfield [1971].
Coal/shale	300,000– 900,000	Yearby [1991].
Sandstone/ limestone	1,000,000– 2,500,000	Yearby [1991].

Additional simple FLAC models calculated the minimum anchor length to hold 100 kN (about 10 tons) without slipping. Again, these models consider a 19-mm bolt of varying length and assumed yield strength for the steel of 200 kN to ensure anchorage slip and not steel failure. Consistent with expectations, the critical anchor length ranged from 1 m at a low Sbond value of 100 kN/m down to 10 cm with a high Sbond value of 1,000 kN/m, as shown in Figure 4. For a given Sbond, a bolt with anchor length more than this critical value will fail by yield of the bolt steel, and with anchor length less than this critical value, anchor slip will occur. Figure 4 suggests that for stronger rocks with Sbond more than 350 kN/m (1 ton/in), short encapsulation pull tests with anchor length of much less than 30 cm (1 ft) are necessary to measure Sbond directly.

INITIALIZATION AND LOADING CONDITIONS

A recent summary of horizontal stress measurements in U.S. coal mines by Dolinar [2003] demonstrated that the horizontal stress magnitude depends on the elastic modulus of the rock layers. Horizontal stress varies according to the relative stiffness of each geologic layer, such that stiff limestone or sandstone layers attract higher horizontal stress than less stiff black shale or claystone layers.

To initialize horizontal stress in a model, the analyst must first calculate the average horizontal strain as

$$\varepsilon_{H\,average} = \frac{\sigma_{H\,average}}{E_{average}} \qquad (3)$$

where $\sigma_{H\,average}$ is the average horizontal tectonic stress and $E_{average}$ is the average modulus. Using Dolinar's approach,

a tectonic strain could also be used directly for the initial far-field boundary condition. Alternatively, if the horizontal stress and modulus are known for a particular layer within a model, the horizontal strain can be calculated on that basis.

Horizontal stress for each layer in the model has a tectonic component and a Poisson component and is calculated as

$$\sigma_{H\,i} = (\varepsilon_{H\,average})(E_i) + \left(\frac{\nu}{1-\nu}\right)(\sigma_{v\,i}) \qquad (4)$$

where E_i is the Young's modulus for a layer, ν is Poisson's ratio, and $\sigma_{v\,i}$ is the vertical stress in a layer. Vertical stress in each layer depends on depth in the usual way. Figure 5 shows a layered model of coal mine rocks initialized with this procedure. Average initial vertical and horizontal stress is 5 and 8 MPa.

PUTTING IT ALL TOGETHER: AN EXAMPLE

This example demonstrates the complete modeling procedure for a coal mine gate road entry in the Pittsburgh Coalbed that is first subject to initial development loading, then additional loading from mining the first longwall panel, and finally more loading as a second longwall panel approaches. Again, Figure 2 shows estimates of axial and diametral point load strength as measured along a core. The point load tests used to estimate the UCS of the rock matrix and the bedding plane strength lead directly to material property assignments based on Tables 1 and 2. Table 5 summarizes a section of the geologic column, strength values from point load tests, and the resulting material property inputs for the model. Figure 5 reflects the layering detail in the overall model. Initial horizontal stress magnitude applied to the model generally correlates to high- or low-strength rock layers. The rock bolts in the model are composed of many sections, where each section corresponds to the top and bottom of a geologic layer. Each bolt section is then assigned an Sbond value consistent with the rock material properties for that layer.

Table 6 indicates the average horizontal and vertical stress applied to the model at different stages. The stresses shown in Table 6 are a two-dimensional approximation to a complex three-dimensional problem. In the gate road development phase, applied stresses are the same as in situ stresses. Mining the first longwall panel effectively induces higher horizontal and vertical stresses far field from the model coal mine entry. The approaching second longwall panel and passage of that second panel induces additional horizontal and vertical stresses. Again, the stress path indicated in Table 6 is only a simple two-dimensional approximation of the actual complex three-dimensional stress field applied to the coal mine entry.

Figure 5.—Initial horizontal stresses. Warm colors indicate high horizontal stress in stiffer layers; cool colors indicate low horizontal stress in less stiff layers. The future entry is shown at center.

Table 5.—Going from core log to numerical model input parameters

Height into roof (m)	Rock type	UCS axial PLT (MPa)	Bedding strength diam. PLT (MPa)	Rock matrix code (Table 1)	Bedding plane code (Table 2)
3.00.....	Sandy bl sh	33.70	12.40	RM5	RBP3
2.90.....	Sandy bl sh	33.70	12.40	RM5	RBP3
2.80.....	Sandy bl sh	33.70	12.40	RM5	RBP3
2.70.....	Sandy bl sh	33.70	12.40	RM5	RBP3
2.55.....	Sandy bl sh	33.70	12.40	RM5	RBP3
2.40.....	Coal	12.00	6.70	CM3	CBP3
2.30.....	Coal	12.00	6.70	CM3	CBP3
2.20.....	Coal	12.00	6.70	CM3	CBP3
2.10.....	Coal	12.00	6.70	CM3	CBP3
2.03.....	Coal	12.00	6.70	CM3	CBP3
1.90.....	Bl sh + coal	18.00	4.00	RM3	RBP2
1.80.....	Bl sh + coal	18.00	4.00	RM3	RBP2
1.69.....	Bl sh + coal	18.00	4.00	RM3	RBP2
1.60.....	Claystone	8.00	2.00	RM2	RBP1
1.50.....	Claystone	8.00	2.00	RM2	RBP1
1.40.....	Claystone	8.00	2.00	RM2	RBP1
1.30.....	Claystone	8.00	2.00	RM2	RBP1
1.18.....	Claystone	8.00	2.00	RM2	RBP1
1.08.....	Black shale	18.00	4.00	RM3	RBP2
0.98.....	Coal	12.00	6.70	CM3	CBP3
0.88.....	Coal	12.00	6.70	CM3	CBP3
0.76.....	Black shale	18.00	4.00	RM3	RBP2
0.64.....	Black shale	18.00	4.00	RM3	RBP2
0.52.....	Coal	12.00	6.70	CM3	CBP3
0.40.....	Coal	12.00	6.70	CM3	CBP3
0.28.....	Black shale	18.00	4.00	RM3	RBP2
0.16.....	Black shale	18.00	4.00	RM3	RBP2
0.00.....	Coal	12.00	6.70	CM3	CBP3

Bl sh = Black shale.   PLT = point load test.

Table 6.—Applied stress path at model boundary

Loading condition	Average horizontal stress (MPa)	Average vertical stress (MPa)
Development	8	5
1st panel mining	14	9
2nd panel mining	17.6	11.4
Postmining....................	20	13

To apply these additional horizontal and vertical stresses to the model, equivalent average strains are calculated based on a weighted average modulus for the model. Based on the overall model dimensions, equivalent displacements at the model boundary are calculated. These displacements are then achieved in the model by slowly applying a velocity at the boundary for a prescribed number of computational steps. Velocity at the model boundary is then set to zero for additional computational steps to achieve equilibrium.

The modeling analyzes two alternative support systems, namely, 2.4-m fully grouted rock bolts alone and with 4-m-long cable bolts. Figure 6 compares these alternatives by showing rock bolt loads, rock bolt anchor slip, rock bolt breakage, and rock mass shear failure superimposed on the UCS of the rock matrix. Different shades represent rock layers of different rock matrix strength. Generally in the Pittsburgh Coalbed, the immediate roof rock is low-strength black shale, thin coal layers, and claystone. Above the immediate roof rock is somewhat higher-strength gray shale and siltstone beds. Rock mass failure has occurred throughout the immediate roof. Zones

of intense bedding plane slip exist above the upper corners of the entry, and these zones propagate 2 to 3 m into the roof. Bedding plane separation has also developed 1.5, 2.5, and 4.5 m into the roof rock, as shown in Figure 7.
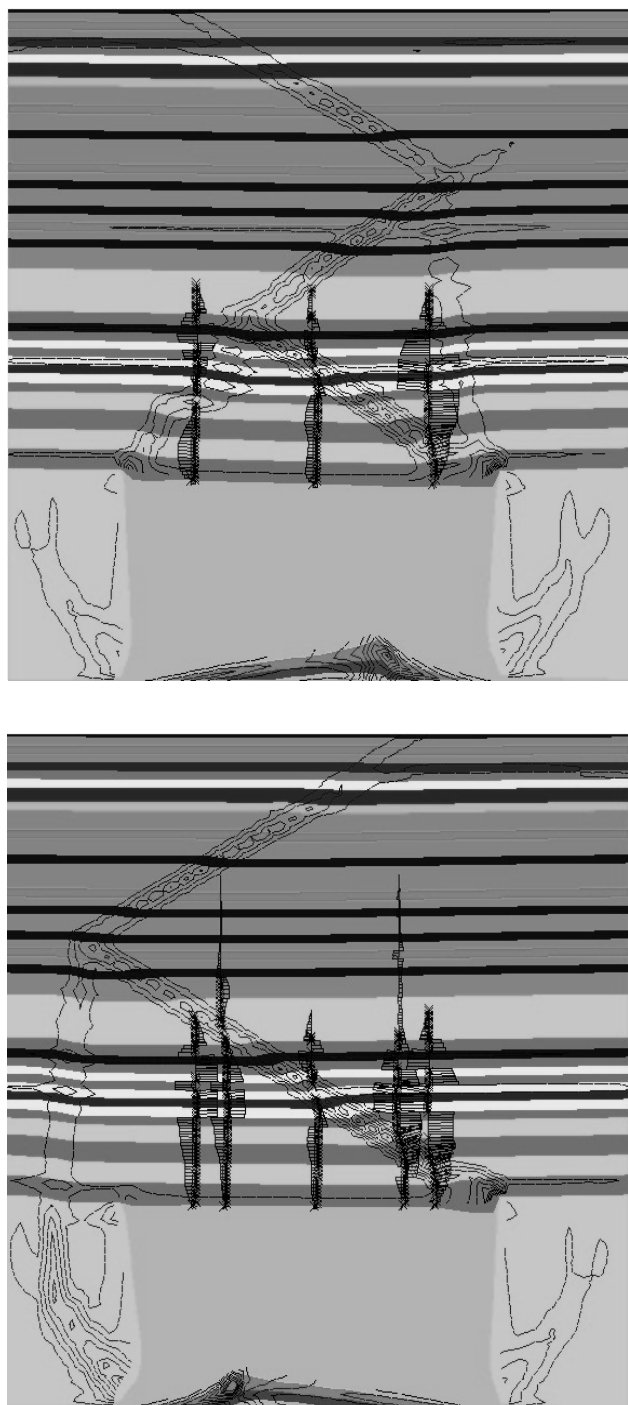

Compressive failure of the immediate roof rock has localized into several "shear bands," as indicated in Figure 6 with the shear strain index parameter in FLAC. These shear bands are more developed with the lighter support system consisting of bolts alone. The failure has also tended to favor one side of the roof more than the other. Downward roof movement is much greater on the left than on the right. The magnitude of rock bolt load is plotted as a percentage of yield strength of the steel. For the untensioned, fully grouted rock bolts used in this model, the load increases from zero at the bolt head, rises to a maximum somewhere in the middle, and decreases back to zero at the anchorage end. The shape of the load profile follows the measured laboratory experiments, as shown in Figure 3. All bolt loads are tensile, no matter whether the load is plotted left or right of the bolt. Anchorage slip is indicated by crosses along the bolt. At the highest load applied to the model, anchor slip has occurred almost everywhere along the rock bolts and the lower portion of the cable bolts. Rock bolt or cable bolt breakage can occur if load on the bolt equals the yield load and if strain in the bolt exceeds 2%. Bolt breakage occurs in the left and center bolts for the bolts-alone case and only in the center bolt if cable bolts are also installed. Although the broken section of bolt is not visible in Figure 6, the low axial loads on either side of the shear zone mark the location of the broken bolt section.

Figure 7 shows the effectiveness of the two alternative rock support systems for controlling immediate roof movement under progressively higher load conditions. Under development conditions with horizontal and vertical stresses of 8 and 5 MPa, respectively, roof displacement is less than 10 mm and both bolt alternatives behave identically. Mining the first longwall panel increases horizontal and vertical stresses to 14 and 9 MPa; however, calculated roof displacements remain under 30 mm, and there is still negligible difference between the two alternatives. When the second longwall panel approaches, the necessity of the cable bolts becomes evident. In the alternative without cables, downward roof displacement at
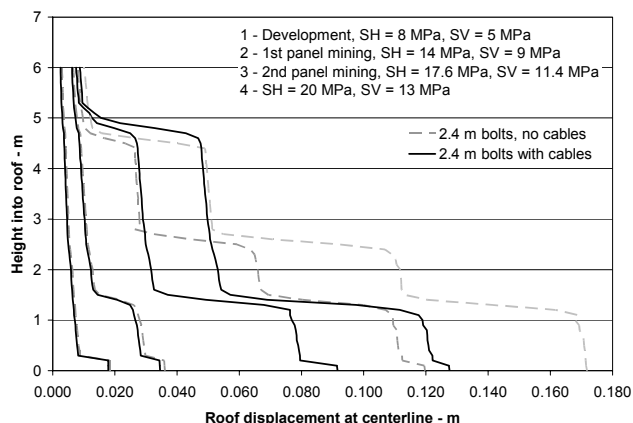

Figure 6.—Support system performance with 2.4-m bolts alone *(top)* **and with 2.4-m bolts with 4-m cables** *(bottom)***. Rock layers of different strength are shaded. Shear zones are contoured. Maximum shear strain contour is 0.5. Rock bolt load is indicated.**

Figure 7.—Immediate roof displacement response for two rock support alternatives.

2-m horizon approaches 70 mm, whereas with cables movement at this horizon is about 30 mm. Total downward roof movement in excess of 50 mm and sudden jumps in that movement with small increases in the applied load on the model are indicative of roof instability and ineffective roof support.

CONCLUSIONS

This paper presents progress toward a standard method for the use of numerical models in practical ground control planning. The method includes procedures for collecting the needed input data, setting up a model, and interpreting the results of calculations.

Collecting the input data needed for a numerical model begins with development of a detailed geologic core log. This core log must capture geologic layers of similar mechanical properties and also note particular features such as exceptionally weak clay layers. Point load testing is a convenient method to estimate the UCS of the rock matrix and the bedding plane strength for each geologic layer.

This paper proposes a suite of material property input parameters aimed at the SU constitutive model in FLAC. This suite of "numerical rocks" includes very weak soils and weak rocks to the strongest rocks found in coal mining. Having estimates of UCS and bedding plane strength for each geologic layer, the user can readily create a numerical model that correctly reflects the geologic situation. The suggested procedure has the distinct advantage of being organized and reproducible. In principle, two different individuals could examine a geologic section, describe it, test it, and develop the same numerical model inputs for the field conditions.

This paper also presents select properties needed to represent rock supports in a numerical model. The significant feature of the rock bolt properties is the linkage between rock bolt anchorage and the specific geologic layer containing that section of the rock bolt. Sections of a rock bolt in weak rocks have low anchor strength and vice versa in stronger rocks.

A practical example of a numerical model that follows the proposed procedure leads to very realistic results. The calculations capture the rock failure process correctly and agree with failure observations in the field. Calculated stresses and displacements in the model are consistent with field measurements of the same.

REFERENCES

Bartels JR, Pappas DM [1985]. Comparative laboratory evaluation of resin-grouted roof bolt elements. Pittsburgh, PA: U.S. Department of the Interior, Bureau of Mines, RI 8924. NTIS No. PB 85–193449.

Dolinar DR [2003]. Variation of horizontal stresses and strains in mines in bedded deposits in the eastern and midwestern United States. In: Peng SS, Mark C, Khair AW, Heasley KA, eds. Proceedings of the 22nd International Conference on Ground Control in Mining. Morgantown, WV: West Virginia University, pp. 178–185.

Dolinar DR, Bhatt SK [2000]. Trends in roof bolt application. In: Mark C, Dolinar DR, Tuchman RJ, Barczak TM, Signer SP, Wopat PF, eds. Proceedings: New technology for coal mine roof support. Pittsburgh, PA: U.S. Department of Health and Human Services, Public Health Service, Centers for Disease Control and Prevention, National Institute for Occupational Safety and Health, DHHS (NIOSH) Publication No. 2000–151, IC 9453, pp. 43–51.

Dunham RK [1974]. Field testing of resin anchored rock bolts. Colliery Guardian *222*:147–151.

Farmer IW [1968]. Engineering properties of rocks. London: E. & F. N. Spon, Ltd.

Farmer IW [1975]. Stress distribution along a resin grouted rock anchor. Int J Rock Mech Min Sci Geomech Abstr *12*:347–351.

Franklin JA, Woodfield PF [1971]. Comparison of a polyester resin and a mechanical rockbolt anchor. Trans Inst Min Metal (Section A: Mining Industry), A91–A100.

Gale WJ, Fabjanczyk MW [1993]. Design approach to assess coal mine roadway stability and support requirements. In: Proceedings of the Eighth Australian Tunneling Conference (Sydney, New South Wales, Australia), pp. 1–7.

Gale WJ, Tarrant GC [1997]. Let the rocks tell us. In: Proceedings of the Symposium on Safety in Mines: The Role of Geology, pp. 153–160.

Hoek E, Kaiser PK, Bawden WF [1995]. Support of underground excavations in hard rock. Rotterdam, Netherlands: Balkema.

ISRM [1981]. Basic geotechnical description of rock masses. International Society for Rock Mechanics.

ISRM [1985]. Suggested methods for determining point load strength. International Society for Rock Mechanics.

ISRM [1993]. Supporting paper on a suggested improvement to the Schmidt rebound hardness ISRM suggested method with particular reference to rock machineability. International Society for Rock Mechanics.

Itasca Consulting Group [1994]. Fast Lagrangian analysis of continua. Minneapolis, MN: Itasca Consulting Group, Inc.

Jaeger JC, Cook NGW [1979]. Fundamentals of rock mechanics. 3rd ed. New York: Chapman and Hall.

Kwitowski AJ, Wade LV [1980]. Reinforcement mechanisms of untensioned full-column resin bolts. Pittsburgh, PA: U.S. Department of the Interior, Bureau of Mines, RI 8439. NTIS No. PB 81–147266.

Mark C, Compton CS, Oyler DC, Dolinar DR [2002]. Anchorage pull testing for fully grouted roof bolts. In: Peng SS, Mark C, Khair AW, Heasley KA, eds. Proceedings of the 21st International Conference on Ground

Control in Mining. Morgantown, WV: West Virginia University, pp. 105–113.

Mark C, Molinda GM, Barton TM [2002]. New developments with the coal mine roof rating. In: Peng SS, Mark C, Khair AW, Heasley KA, eds. Proceedings of the 21st International Conference on Ground Control in Mining. Morgantown, WV: West Virginia University, pp. 294–301.

Medhurst T, Hatherly P [2005]. Geotechnical strata characterization using geophysical borehole logs. In: Peng SS, Mark C, Tadolini SC, Finfinger GL, Khair AW, Heasley KA, eds. Proceedings of the 24th International Conference on Ground Control in Mining. Morgantown, WV: West Virginia University, pp. 179–186.

Molinda GM, Mark C [1996]. Rating the strength of coal mine roof rocks. Pittsburgh, PA: U.S. Department of the Interior, Bureau of Mines, IC 9444. NTIS No. PB96–155072.

Pettibone HC [1987]. Avoiding anchorage problems with resin-grouted roof bolts. Spokane, WA: U.S. Department of the Interior, Bureau of Mines, RI 9129. NTIS No. PB 88–230172.

Reddish DJ, Whittles DN, Stace LR [2000]. The application of rock classification principles to coal mine design in U.K. conditions. In: Peng SS, Mark C, eds. Proceedings of the 19th International Conference on Ground Control in Mining. Morgantown, WV: West Virginia University, pp. 348–357.

Rusnak J, Mark C [2000]. Using the point load test to determine the uniaxial compressive strength of coal measure rock. In: Peng SS, Mark C, eds. Proceedings of the 19th International Conference on Ground Control in Mining. Morgantown, WV: West Virginia University, pp. 362–371.

St. John CM, Van Dillen DE [1983]. Rockbolts: a new numerical representation and its application in tunnel design. In: Proceedings of the 24th U.S. Symposium on Rock Mechanics. New York: Association of Engineering Geologists, pp. 13–26.

Serbousek MO, Signer SP [1987]. Linear load-transfer mechanics of fully grouted roof bolts. Spokane, WA: U.S. Department of the Interior, Bureau of Mines, RI 9135. NTIS No. PB 88–230230.

Signer SP [1990]. Field verification of load-transfer mechanics of fully grouted roof bolts. Spokane, WA: U.S. Department of the Interior, Bureau of Mines, RI 9301. NTIS No. PB 90–225871.

Tadolini SC [1986]. Anchorage capacities in thick coal roofs. Denver, CO: U.S. Department of the Interior, Bureau of Mines, IC 9058. NTIS No. PB 86–169174.

Yearby M [1991]. Practical guide to rock bolting. Newcastle, New South Wales, Australia: ANI Arnall, Ltd.

NIOSH

Delivering on the Nation's promise:

Safety and health at work for all people through research and prevention

To receive documents or more information about occupational safety and health topics, contact NIOSH at

1–800–35–NIOSH (1–800–356–4674)
Fax: 513–533–8573
E-mail: pubstaft@cdc.gov

or visit the NIOSH Web site at www.cdc.gov/niosh

SAFER • HEALTHIER • PEOPLE ™